Structure Optimization of Polycaprolactone Foams by Using Mixtures of CO_2 and N_2 as Blowing Agents

E. Di Maio, G. Mensitieri
Department of Materials and Production Engineering, Faculty of Engineering, University of Naples Federico II, P.le Tecchio 80, 80125 Naples, Italy

S. Iannace, L. Nicolais
Institute of Composite and Biomedical Materials (IMCB-CNR), National Research Council of Italy, P.le Tecchio 80, 80125 Naples, Italy

W. Li, R.W. Flumerfelt
Department of Chemical Engineering, University of Houston, 4800 Calhoun Road, Houston, Texas 77204

The foaming process of poly(ε-caprolactone) (PCL) with carbon dioxide and nitrogen has been investigated in this work from a theoretical and experimental point of view. CO_2 and N_2 showed very different behavior, as foaming agents for PCL. This was due to the different transport, chemical, and physical properties of the polymer/gas mixture that led to different foam morphology in terms of density, cell number density, and cell size. The lowest density (0.03 g/cm^3) was obtained with CO_2, but the highest number of cells with N_2 (although with a higher density, (0.2 g/cm^3). Foam with a low-density microcellular structure, was obtained when a mixture of the two gases was employed. POLYM. ENG. SCI., 45: 432–441, 2005. © 2005 Society of Plastics Engineers

INTRODUCTION

Polymeric foams represent an important class of materials with important technological applications. Due to their peculiar properties, these materials find wide use when good mechanical properties and low weight need to be coupled for acoustic insulation and damping, thermal insulation and impact resistance. They can be prepared from virtually any polymer by introducing or generating a gas in a polymeric matrix but suitable materials for industrial foaming applications must possess adequate properties, and the manufacture process must be easy and economic.

Thermoplastic foams can be produced by using continuous or discontinuous technologies, such as extrusion, injection molding, batch foaming, salt leaching, and phase inversion. From the industrial point of view, only extrusion and injection molding are interesting, since the productivity of the other processes is, in general, very low [1–3].

The basic mechanism of foam formation is similar in the extrusion, injection molding, and batch foaming processes. The foamed structure is obtained through a nucleation and growth mechanism of a polymer/gas solution, induced by an abrupt pressure drop, which brings about a super saturation.

Batch foaming and extrusion, due to a better control of the relevant variables, allow an easier study of the foaming process. In effect, the manufacture of foamed products requires a careful selection of the proper combination of polymer/foaming agent system and the proper coordination of the individual steps in the process. The optimization of the foaming process involves the control of the fluidodynamic behavior of macromolecular viscoelastic materials containing a dissolved gas at high concentration and at thermodynamic conditions able to promote the formation of gas bubbles in the melt. Nucleation and growth rates, which determine the final morphology of the foam, are related to the chemical, physical and transport properties of the polymer-foaming agent system: surface and rheological properties of the polymer/gas solution, solubility and diffusivity of the gas into the melt.

In order to form polymeric foam, bubbles must first nucleate and grow within the molten or plasticized viscoelastic material. Subsequently, setting of the structure must occur due to the increase of viscosity during cooling and/or reduction of plasticization and finally solidification of the continuous phase.

The initial nucleation is induced by a change in thermodynamic conditions, generally a change of temperature and/or pressure. During this stage, a second phase is generated from a metastable polymer/gas homogeneous mixture. Based on the classical homogeneous nucleation theory,

Correspondence to: E. Di Maio; e-mail: edimaio@unina.it
DOI 10.1002/pen.20289
Published online in Wiley InterScience (www.interscience.wiley.com).

macroscopic properties such as solubility (S), diffusivity (D), gas concentration (c), surface tension (σ), temperature, and degree of supersaturation are the parameters controlling the nucleation rate (J). There are several equations proposed for J [4–8], and they can be summarized in the following general expression:

$$J = MB \exp\left[- \frac{16\pi\sigma^3}{3k_B T(P_V - P_L)^2} \right] \quad (1)$$

where M and B are increasing functions of the gas concentration, c, and of the gas diffusivity D, respectively. k_B is the Boltzmann constant, and P_V and P_L are the equilibrium gas pressure and the pressure in the liquid phase, whose difference describes the supersaturation of the expanding gas in the solution.

Once the bubble is nucleated, it will grow due to the diffusion of the gas molecules from the solution to the gas phase nucleated. The phenomena governing the expansion of the bubble will therefore be related to the transport properties of the gas in the polymeric melt and to the rheological and surface properties of the matter around the bubble. Isothermal bubble growth is then modeled by the following differential equations [9–13]:

$$\frac{d}{dt}(\rho_G R^3) = 3\rho D R^2 \left(\frac{\partial c}{\partial r} \right)_{r=R} \quad (2)$$

$$\frac{\partial c}{\partial t} + v_r \frac{\partial c}{\partial r} = \frac{D}{r^2} \frac{\partial}{\partial r} \left(r^2 \frac{\partial c}{\partial r} \right) \quad (3)$$

$$\rho \left(\frac{\partial v_r}{\partial t} + v_r \frac{\partial v_r}{\partial r} \right) = - \frac{\partial P}{\partial r} + \frac{1}{r^2} \frac{\partial}{\partial r} (r\tau_{rr}) - \frac{\tau_{\theta\theta} + \tau_{\phi\phi}}{r}. \quad (4)$$

Equations 2–4 are the mass balance in the bubble, the mass balance in the melt, and the momentum balance in the melt, respectively. Here, ρ_G is the gas density inside the bubble, R is the bubble radius, ρ is the fluid density, c is the gas concentration, r is the radial coordinate, v_r is the fluid velocity in the radial direction, P is the fluid pressure, and τ_{ii} are the normal stresses. For the solution of these three equations, it is necessary to know how mass transport properties, rheological description of the stress components, and thermodynamic properties (i.e., surface energy and solubility) depend upon the gas concentration.

These models for nucleation and growth suggest some directions for improving the cellular structure when, as often happens with conventional nonfoamable polymers (like biodegradable, aliphatic polyesters), it is not possible to achieve fine structures and/or low densities. This is often due to the low melt strength of these polymers, which are not able to withstand the elongational stresses acting on cell walls. In this case the collapse and the loss of the expanding gas do not permit the formation of low density materials with uniform cellular morphology.

By analyzing *Eq. 1*, it becomes clear that, given the material to be foamed and the blowing agent, more cells (which means finer morphology) can be simply obtained by increasing the pressure drop, $(P_V - P_L)$, responsible for the nucleation. In the batch process, high pressure drop can be achieved by increasing the saturation pressure. In the extrusion process, instead, this can be achieved independently of the pressure of the foaming gas by controlling the geometry of the dies or channels, where nucleation takes place. Another important parameter determining foam morphology is the foaming temperature. It is not, however, possible to use a wide range of foaming temperatures, as too low temperatures lead to foams with good morphology but higher density, while high temperatures lead to cell collapse. Moreover, it is difficult to achieve an effective control of the cell growth phenomena by acting on the temperature control because the real process is more complex than that depicted by the model equations. Actually, one operates by just imposing a temperature quench on the foamed structure in order to limit the cell collapse [14–23].

Park et al. [24] and Park [25, 26] proposed an efficient method to enhance the foamability of polymers, improving the cellular structure of the foams, by controlling not only the pressure drop, but also the pressure drop rate, that is the rate at which the pressure quench is performed. Their results are easily rationalized based on the fact that nucleation and growth compete in subtracting the expanding gas from the molten polymer/gas solution and that if growth is allowed, no further nucleation can take place around the growing bubble. By maximizing the pressure drop rate, one minimizes the expanding gas loss for the growth and maximizes the cell number density.

Therefore, in order to obtain the highest number of cells and the lowest density it is necessary to increase as much as possible the pressure drop and pressure drop rate and to set temperatures and blowing agent concentration in order to reach a compromise between morphology and density. A maximum limit to the operative pressure may be imposed by the occurrence of melt instabilities.

In this article, we describe the methods utilized to prepare cellular polymers from a biodegradable polyesters, poly(ϵ-caprolactone) (PCL), using both continuous (extrusion) and batch processes. Optimization of the foaming process will be discussed based on the use of a proper mixture of blowing agents, CO_2 and N_2 characterized by very different interactions with the polymer.

MATERIALS AND METHODS

PCL was kindly supplied by Solvay Interox Ltd. (PCL CAPA 6800). Some characteristics of the polymer used were: Mw = 80,000 ca., $T_g = -60$°C, $T_m = 60$°C, $T_c = 30$°C, Young Modulus = 450 MPa. Commercial purity grade CO_2 and N_2 were used as foaming agents.

Gas transport and equilibrium sorption properties were obtained using two different balances, a Cahn D110 mi-

crobalance and a quartz spring balance; the details of the techniques are described elsewhere [27, 28].

For the preparation of foam samples in the batch vessel (a thermoregulated and pressurized cylinder having a volume of 0.5 L), typical experiments were conducted using the following procedure: PCL cylinders 5 mm thick, with a diameter of 10 mm were saturated at 70°C with the foaming agent for at least 6 hours. The saturation pressure, P_{sat}, varied in the range 30–170 bar, depending on the type of gas employed. The vessel was then cooled to the foaming temperature, T_{foam}, and finally pressure-quenched to ambient pressure, using different pressure drop rates. The pressure discharge system was designed to allow three different pressure drop rates. The discharge valve (HiP ball valve, model 15-71 NFB) of the pressure vessel was connected to tubes of different length and/or diameter, in order to change the pressure losses and, therefore, the pressure drop rates. The pressure history was then measured by using a data acquisition system. The effect of the variables such as foaming temperature, foaming agent concentration and pressure drop rate on the foam properties was investigated.

The continuous extrusion process was also used to produce foams. The extrusion line was equipped with special devices in order to obtain a better control of the whole foaming process. According to the suggestions proposed by the works of the MIT group on microcellular foams [7, 8, 24, 27, 29–31], a hot heat exchanger, a nucleation nozzle, and a cold heat exchanger were designed and added to a lab-scale twin screw extruder (Haake CTW100). The functions of these devices are respectively to enhance the foaming agent solubilization, to control the pressure drop and pressure drop rate and to cool the polymer/gas solution to the optimum T_{foam} before the die exit. A mass flow controller (Brooks Instr. 5850S) was used to meter the physical foaming agent (PFA) into the barrel, while venting screws, designed to induce the formation of the so-called dynamic seals, were used to avoid the PFA loss from the hopper.

Monitoring of pressure and temperature was carried out at five points on the extrusion line to allow the optimization of each step of the extrusion-foaming process.

A capillary device, positioned beyond the static mixer, was used to measure the inline shear viscosity of the polymer/gas solution, by measuring the pressure drop across the capillary. Different capillary geometries and different volumetric flow rates of the molten polymer/gas solution were used [32, 33].

The densities of the foamed PCL samples were determined by weighting in water and in air, using a balance with a resolution of 10^{-4} g, according to ASTM D792.

For microstructural analysis, the foamed samples were analyzed by SEM. The samples were first sectioned in liquid nitrogen and then coated with gold using a sputter coater (Emscope SC500). The morphology of the fracture surface was studied by using a LEICA mod. S440 scanning electron microscope operating at 20 kV.

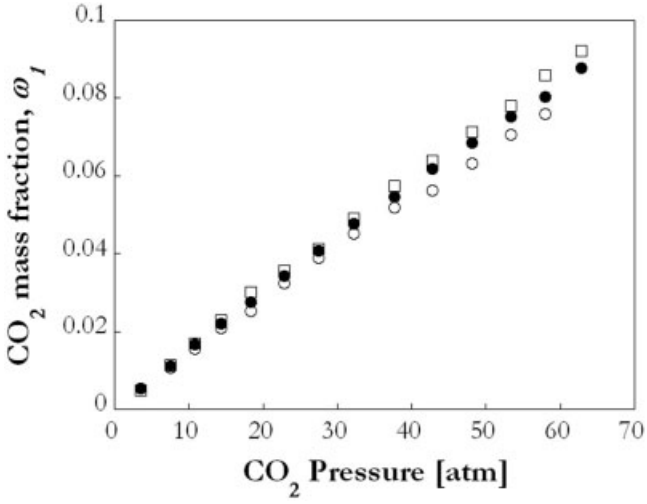

FIG. 1. Sorption isotherms for the PCL/CO_2 system: (□) 70 °C; (●) 75 °C; (○) 85 °C.

RESULTS AND DISCUSSION

Physical and Rheological Properties of PCL/Gas Mixtures

Equilibrium sorption concentrations of CO_2 in PCL at different pressures and temperatures are reported in Fig. 1. As expected, the weight fraction of sorbed CO_2 increases with pressure and decreases with temperature. Figure 2 shows the results of sorption measurements performed with CO_2, N_2 and a 50%wt mixture of CO_2 and N_2 at 75°C. The solubility of CO_2 is higher than N_2. Since the solubility of the mixture is a weighted mean of the solubility of each component, it can be assumed that, for the investigated gas mixtures composition and pressures, there is no interaction between the solubilized gases.

Different mutual diffusivities were evaluated for PCL-CO_2 and PCL-N_2 systems. In fact, PCL-N_2 mutual diffu-

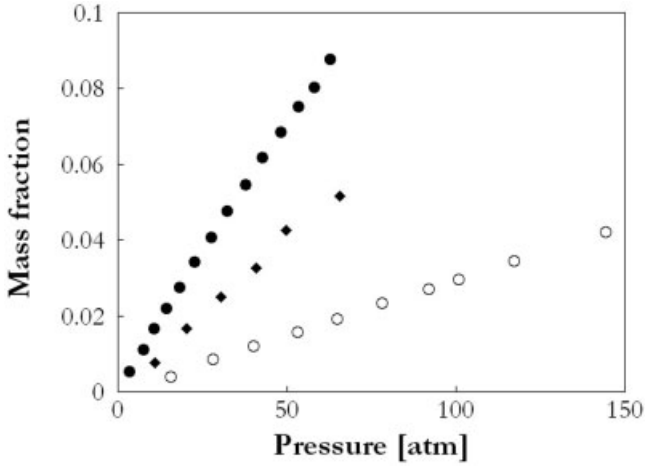

FIG. 2. Sorption isotherms at 75°C for the PCL and different gases: (●) CO_2; (○) N_2; and (◆) 50 wt% CO_2/N_2 mixture.

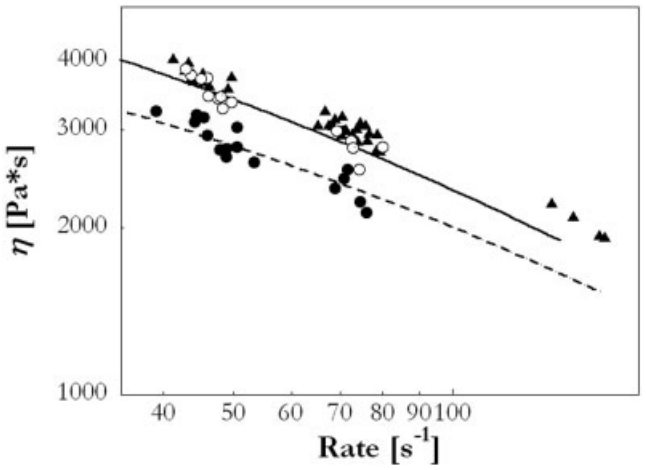

FIG. 3. Rheological properties of the PCL-gas systems at 100°C: (continuous line) pure PCL, capillary rheometer; (▲) pure PCL, inline measurements; (●) PCL + 2.3 wt% CO_2, inline measurements; (○) PCL + 1.5 wt% N_2, inline measurements; (dashed line) prediction of the model (see text for details).

sivity (data not reported) is more than one order of magnitude higher than PCL-CO_2 (28). This difference, according to *Eq. 1*, will result in a dramatic difference in the nucleation phenomena of the polymer-gas mixture, as will be discussed later.

Another important difference between the two foaming agents is related to the plasticization effects on PCL. It is well known that certain compressed gases can dissolve to considerable extents in polymers causing a depression in the glass transition and crystallization temperatures [34, 35]. The increase of free volume, which accompanies plasticization, leads to an increase of molecular mobility and therefore to a decrease of the melt viscosity and of the surface tension of the system, to an extent that depends on the gas concentration and on the interaction between the polymer and the gas. This phenomenon is very important, since it can affect the cell growth and can reduce foam mechanical stability, due to the decrease of the melt strength of the polymer. In Fig. 3, results of the inline shear viscosity measurements of the PCL/CO_2 and PCL/N_2 systems are reported. The comparison between carbon dioxide and nitrogen was performed at the same molar concentration of gas and shows that the reduction of viscosity is more pronounced in presence of CO_2.

The plasticization effect of the PFA on the molten polymer can be described by two contributions: a dilution effect (the viscosity of the solution is a weighted mean of the viscosities of the two components) and a free volume increase effect (the PFA is responsible for the increase of the specific free volume of the molten polymer). As reported by various authors [32, 36] viscosity-frequency spectrum of the polymer-PFA solution is similar to the one of the pure polymer and a shift factor approach can be used. Therefore the plasticizing effect can be described by the following:

$$\eta(\dot{\gamma}, e) = \eta(a\dot{\gamma})*a,$$

with

$$a = (1 - \omega_1)^n \left(\frac{V_p}{V_m}\right)^n \exp\left(\frac{1}{f_m} - \frac{1}{f_p}\right), \quad (5)$$

where: e is the PFA concentration; η is the viscosity of the pure polymer and of the solution; a is the scaling factor; ω_1 is the weight fraction of the gas; V_p and V_m are the polymer and mixture specific volumes; f_p and f_m are the polymer and mixture fractional free volumes; and n is the exponent for the dilution effect term.

In this work, ω_1 is imposed (solubility in the nucleation device, mass fluxes in the extruder); V_p is known from the *PVT* data on the PCL [28]; V_m has been theoretically evaluated using the equation of state (EOS) theories for mixtures introduced by Simha and Somcinsky (SS-EOS) [37, 38]; f_p and f_m have been computed using the fractional free volume defined by the SS-EOS [37–39] as better detailed in the following; and finally n, as suggested by Gerhardt et al. [32], has been assumed to range from 3 to 3.5 (a value of 3.5 has been used) and its effect is quite negligible in comparison to the exponential term in *Eq. 5*.

Another important effect on the viscosity is related to pressure that counteracts the plasticization of the molten polymeric phase induced by PFA. In fact, an increase of pressure promotes a depression of free volume, favoring the increase of viscosity. Also this effect can be simply taken into account using the free volume prediction of the EOS for the PFA-PCL mixture. As a consequence, changes of viscosity can be predicted by using a more general expression for the shift factor that in the exponential term takes into account both the effect of concentration and pressure on free volume, which is evaluated from EOS theory for the mixture. It is worth noting that also the value of V_m, which is evaluated using EOS as well, accounts for the effects of concentration of dissolved PFA and of pressure. The effect of pressure on V_p has been measured using the experimental apparatus for *PVT* properties of pure polymer [28]. Actually pressure is not constant in the inline capillary rheometer, hence for the sake of simplification, an average pressure $\bar{P}$ in the capillary has been used to evaluate a, V_m, and V_p.

Finally, for the PCL/CO_2 system the different terms were calculated as follows:

- For pure PCL: T = 100°C, $\bar{P}$ = 40 bar, V_p = 0.9609 cm^3/g, from experimental data (T is set in the capillary zone of the extrusion line, $\bar{P}$ is the mean pressure inside of the capillary, V_p is measured by *PVT* tests; f_p = 0.1049, obtained by fitting the experimental *PVT* data with the SS-EOS for pure polymer and extracting the free volume fraction ($f_p = 1 - y$), where y is the fraction of occupied lattice sites [37, 38].
- For mixture with ω_1 = 2.3 wt% of CO_2 (value that has been set by fixing the mass flow of the two species): T = 100°C, $\bar{P}$ = 80 bar, from experimental, extrusion data; and V_m = 0.9585; f_m = 0.1092, obtained by predicting the data with the SS-EOS.

From those values, by using *Eq. 5*, we calculated a value for a equal to 0.64, which has been used to predict the viscosity of the PCL/CO_2 solution reported in Fig. 3. It is worth noting that: 1) no fitting parameters were used, since the SS-EOS characteristic parameters of both pure polymer and penetrant were known, and 2) that the predicted rheological properties of the solution are in good agreement with the experimental data.

Another important effect of the PFA is the depression of the characteristic temperatures of the polymer/gas solution, with respect of the pure polymer. In effect, as reported for several polymers such as poly(ethylene terephthalate) (PET), poly(methyl methacrylate) (PMMA) [34, 35, 40], poly(ether-ether-ketone) (PEEK) [41], polycarbonate (PC) [42], and syndiotactic polystyrene (sPS) [43], the presence of gas can depress the crystallization and melting temperatures and modify the crystallization kinetic of the polymer to an extent that, again, depends on the quantity and the kind of the gas. For example, CO_2 was found to induce a remarkable decrease of the melting temperature of sPS, while compressed N_2, under similar pressures was found to have no effects [43, 44].

Similar results were found in the present investigation for the use of PCL. When the polymer was foamed with CO_2 in the pressure vessel (batch foaming apparatus) it was possible to reduce the foaming temperature (T_{foam}) down to 27°C, due to the depression of the crystallization temperature induced by the gas (as evaluated by a DSC test, when cooling the pure PCL from the melt at 10°C/min, the measured crystallization temperature is about 30°C). When the foaming agent was N_2, the lowest temperature that could be employed was 45°C. At lower temperatures, the crystallization process of the polymer was too fast and the pressure developed in the nucleated bubbles was not enough for the expansion of the structure.

As already discussed, the polymer melt surface tension also plays an important role in bubble nucleation and growing. The surface tension of a polymer-gas solution is lower than that of the pure polymer and it is a strong function of the polymer-gas systems and gas concentration. In the view of the higher solubility of CO_2 in the PCL melt the surface tension of the PCL/CO_2 system is expected to be lower than in the case of the N_2/PCL solution, as reported also for PS systems [45].

In the hypothesis that both surface tension and viscosity of the PCL/CO_2 system are lower than those of the PCL/N_2 system, one would expect an easier growth of the bubbles when using CO_2 on the basis of *Eq. 4*. In fact, in this case, the normal stresses (exerted by the viscous forces in the bulk and by the surface forces at bubble surface) which work against the growth of the bubbles are lower. This, in conjunction with a higher solubility of carbon dioxide with respect to nitrogen, will lead, as described in the following, to foams of lower densities for PCL/CO_2 system with respect to PCL/N_2 system.

TABLE 1. PCL-CO_2 batch-foaming experimental data.

Test no.	T_{foam} (°C)	t_{foam} (s)	P_{sat} CO_2 (bar)	d (g/cm^3)
1	39.4	6	55	0.043
2	29.4	6	55	0.116
3	29.4	6	55	1[a]
4	35.0	6	55	0.050
5	32.2	6	55	0.075
6	35.0	4	55	0.053
7	32.2	4	55	0.060
8	29.4	4	55	0.104
9	32.2	4	55	0.084
10	27.2	4	55	0.285
11	27.2	2	55	0.231
12	32.2	2	55	0.088
13	29.4	2	55	0.102
14	32.2	2	55	0.056
15	29.4	2	55	0.099
16	27.2	2	55	0.125
17	29.4	2	55	0.085
18	29.4	2	41	0.143
19	29.4	2	41	0.164
21	29.4	2	41	0.177
22	29.4	2	48	0.103
23	27.2	2	34	0.185
24	29.4	2	34	0.164
25	35.0	2	28	0.110
43	43.3	2	28	1[b]
44	37.8	2	28	1[b]
45	32.2	2	28	0.244
46	32.2	2	28	0.285
47	28.9	2	28	1[c]
51	29.4	2	59	0.046
52	32.2	2	59	0.033

[a]First cooled to 20°C and then re-heated to reach T_{foam}.
[b]Intense collapse.
[c]Not expanded.

Batch Foaming

PCL/CO_2 System. Table 1 reports the experimental conditions used for the preparation of PCL foams with CO_2. The samples prepared at $T_{foam} > 35$°C and pressure drop rate equal to 10 bar/s (#1–#5) showed a cellular morphology characterized by few bubbles of great size (Fig. 4). In fact, at these temperatures, PCL was not able to crystallize and the low viscosity of the cell wall material did not permit a complete stabilization of the cellular structure, and coalescence phenomena likely occurred.

An improvement in the cellular morphology was obtained by raising the pressure gradient up to 30 bar/s and by lowering T_{foam}. As an example, comparison of foams morphologies produced at the same saturation pressure and at the same temperature but with different pressure drop rate is shown in Fig. 5. Higher pressure drop rate resulted in foams of finer morphology, with a higher cell density and smaller size (#11–#22). In this case, the higher drop rate led to materials of lower density, since the loss of gas was limited by the fine morphology of the cellular structure. The lowest density (0.03 g/cm^3) was achieved at $T_{foam} = 32$°C, $P_{sat} = 59$ bar and pressure

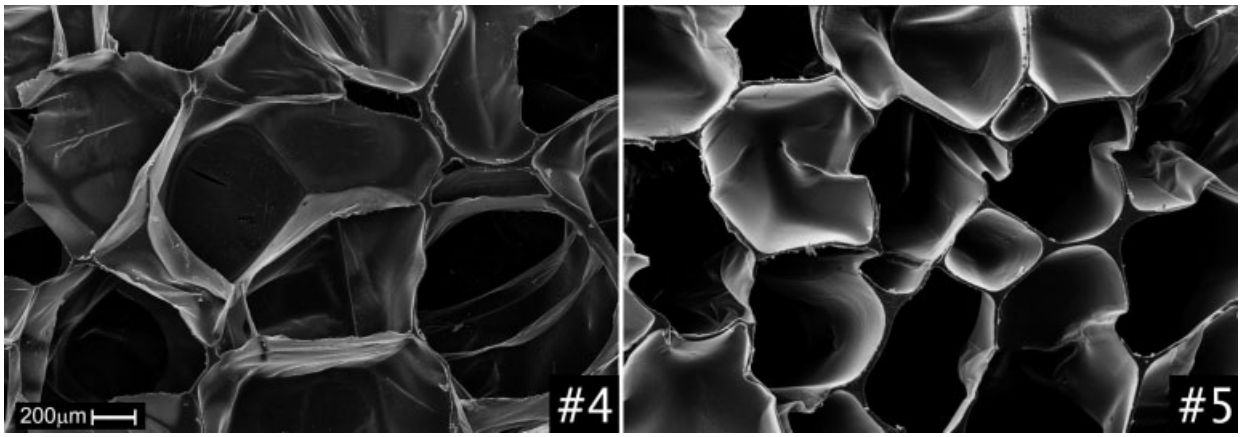

FIG. 4. SEM analysis of PCL batch-foamed with CO_2, high temperatures and low pressure drop rate (refer to Table 1 for numbering).

drop rate of 30 bar/s (sample #52). The mean diameter of the cells was 250μm.

The density measurements were performed right after the complete solidification of the samples and were repeated after 1 day, to study the aging of the structure. The densities were found to be significantly higher in the latter case, in some cases up to 200% (the values reported in Table 1 refer to the measurements performed after one day). This was due to the contraction of the cellular structure caused by the loss of CO_2 through the solidified cell walls indicating that, at room temperature, the diffusivity of CO_2 in PCL is high enough to permeate in few hours. Since the loss of gas due to the permeation through the cell walls did not cause their rupture, the physical collapse of the structure was related, in this case, to the reduction of the pressure within the bubbles. This contraction is quite evident in Fig. 4, in particular in test #5, where cell walls folding (and not rupture) can be observed.

To prevent the collapse during the depressurization phase, lower concentration of the dissolved gas and hence lower saturation pressure should be used, to induce a higher density of the foam. However, it should be considered that in a batch process pressure drop rate and gas saturation pressure cannot be changed independently. In fact a lower saturation pressure is accompanied by a lower pressure drop rate which, in turn, promotes a poorer final morphology, as discussed above. Consequently, optimal foaming conditions in a batch apparatus, aimed to the achievement of a good morphology, derive from a compromise of these two aspects. Conversely, in the extrusion processes, where the pressure drop does not depend on the saturation pressure but on the geometry of the nucleation nozzle and on the volumetric flow rate, the decrease of gas concentration is possible and leads to stable, relatively high-density PCL/CO_2 foams.

PCL/N_2 System. The morphologies of foams prepared with N_2 as foaming agent are reported in Fig. 6. The experimental foaming conditions are reported in Table 2. Foaming, in this case, was performed at temperatures higher than in the case of CO_2. In fact, it was not possible to perform the foaming process at $T_{foam} < 43$°C. This is due to the lower solubility and to the negligible plasticizing effect of N_2. The lower concentration of dissolved gas promoted

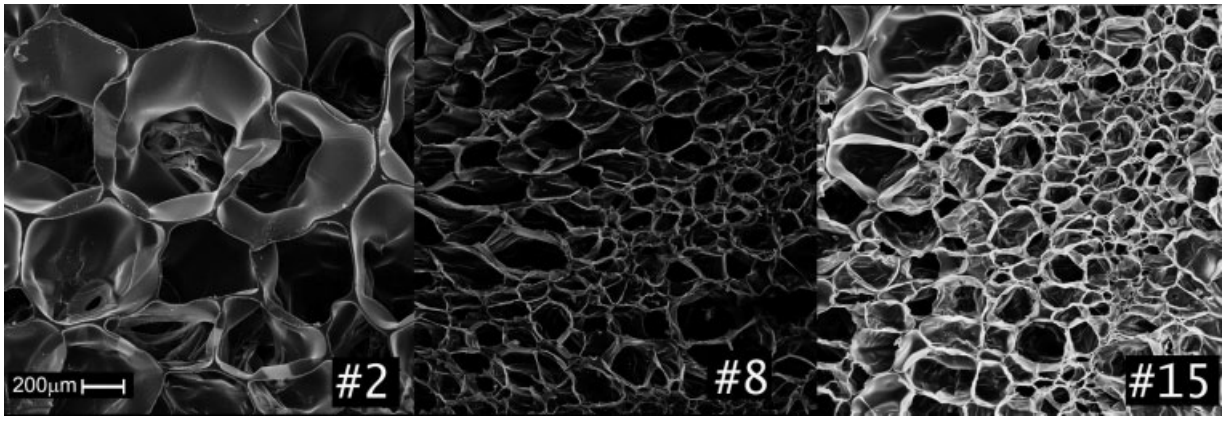

FIG. 5. SEM analysis of PCL batch-foamed with CO_2, effect of the pressure drop rate (refer to Table 1 for numbering).

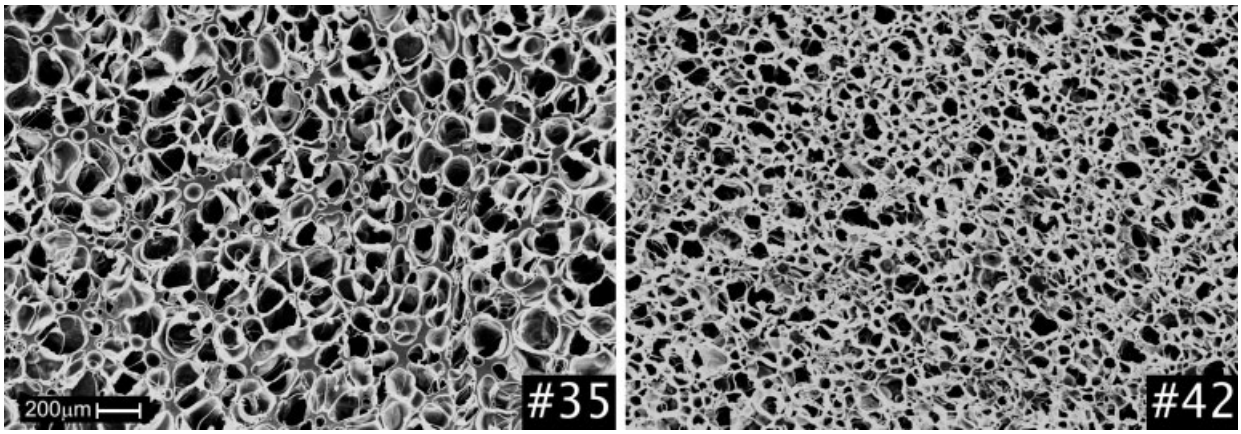

FIG. 6. SEM analysis of PCL batch-foamed with N_2 (refer to Table 2 for numbering).

foam densities higher than those obtained with CO_2. On the other hand, the higher saturation pressures (and the higher pressure drop rates) led to a very fine structure. So-called microcellular foams were obtained at $T_{foam} = 43°C$, $P_{sat} =$ 170 bar, and pressure drop rate of 80 bar/s, with a cell diameter of about 20 μm (#42).

In contrast with CO_2-foamed PCL, the foam contraction did not take place since the higher densities and the fine morphologies led to very rigid structures.

PCL/CO_2/N_2 System. From the above results we concluded that tailoring of cellular structures could be obtained by combining the effects of the two gases, by using a CO_2-N_2 mixture as foaming agent. In fact, CO_2 was found to be a good foaming agent due to the high solubility and the high plasticizing effects while N_2 led to a better morphology in terms of cell size and number density. Foams with different density and number cell density were obtained by using different compositions of CO_2/N_2 and different saturation pressures (see Table 3). In this case a little amount of CO_2 was enough to inflate the high number of bubbles generated by N_2 and to achieve foams with a very fine morphology and low densities at the same time. A comparison of several foams is reported in Fig. 7. The foaming temperatures were intermediate between the foaming temperatures of the two pure gases, suggesting that the plasticizing effect could, in this gross evaluation, be considered additive.

TABLE 2. PCL-N_2 batch-foaming experimental data.

Test no.	T_{foam} (°C)	t_{foam} (s)	P_{sat} N_2 (bar)	d (g/cm^3)
20	29.4	2	90	1[a]
26	40.0	2	138	1[a]
27	47.8	2	103	1[a]
28	60.0	2	103	1[b]
29	54.4	2	103	1[b]
30	43.3	2	172	0.41
31	48.9	2	145	1[b]
32	52.8	2	124	0.64
33	48.9	2	103	1[b]
34	51.7	2	117	1[b]
35	48.9	2	172	0.19
42	43.3	2	172	0.24

[a]Not expanded.
[b]Intense collapse.

Extrusion Foaming

The continuous extrusion process is important to achieve industrial productivity. Until now, little interest has been given to biodegradable polyesters, mostly because they are considered, in general, not foamable, due to poor properties of the melt. In fact results of the batch foaming suggested that it is possible to overcome this problem by controlling and improving the whole foaming process. The extrusion foaming is characterized by the same intense collapsing, density, and morphology issues as in the case of batch foaming and the methods to be used to improve the quality of extruded foams are analogous.

While evolution of a foaming and control of the batch process occurs on a time coordinate, in the case of the extrusion, the process occurs on a spatial coordinate, i.e., along the screw axis. In the first three screw zones, we have melting, gas injection, solubilization, and pressurization. In

TABLE 3. PCL-CO_2/N_2 batch-foaming experimental data.

Test no.	T_{foam} (°C)	t_{foam} (s)	P_{sat} CO_2 (bar)	P_{sat} N_2 (bar)	d (g/cm^3)
36	29.4	2	48	90	0.51
37	32.2	2	48	90	0.07
38	32.2	2	55	55	0.23
39	35.0	2	34	55	0.13
40	40.6	2	17	55	0.34
41	40.6	2	17	121	0.15
48	40.6	2	7	83	1[a]
49	40.6	2	10	138	0.24
50	37.8	2	48	76	0.07

[a]Not expanded.

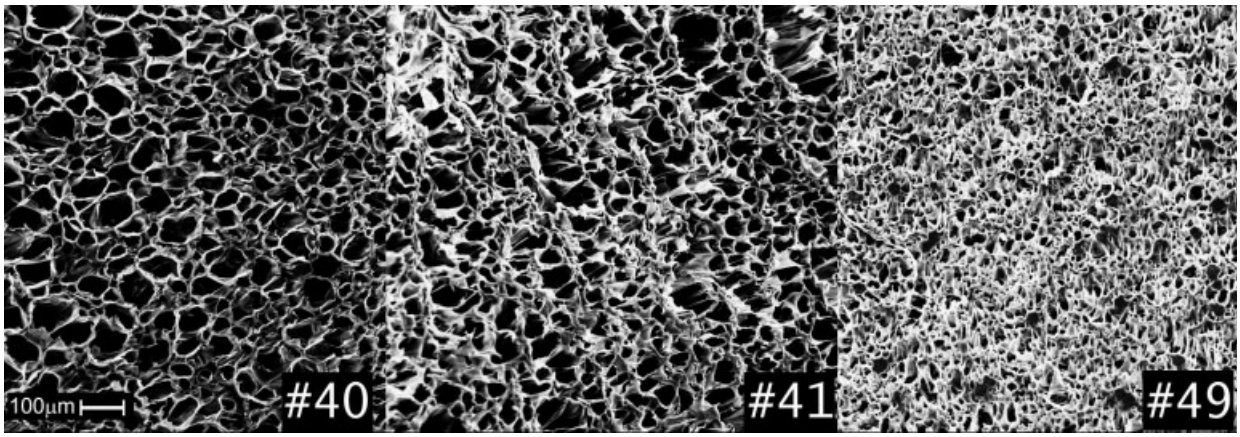

FIG. 7. SEM analysis of PCL batch-foamed with the CO_2/N_2 mixtures (refer to Table 3 for numbering).

the static hot mixer, further solubilization is allowed by increasing the residence time and contact between the two phases. When the solubilization step is complete, the polymer/gas solution is forced to pass through a narrow capillary (referred to as the nucleation nozzle), where the pressure drop promotes nucleation. By changing the pressure drop and the pressure drop rate, it is possible to control cell morphology. A fast and intense pressure drop gradient has to be imposed on the flowing polymer/gas solution to improve the cell structure and reduce cell collapse. Finally the nucleated system is cooled to T_{foam} and exits the die, allowing complete growth. The foaming temperature must be set in order to obtain the optimal compromise between density and collapse. In fact, a higher temperature allows a complete diffusion of the gas from the solution to the growing bubble, leading to a complete morphology evolution, but reduces the melt strength, which can favor coalescence and/or collapse of the cellular structure. On the other hand, lower temperatures can limit the cell growth, with a reduction in foaming efficiency.

Even if the batch process has provided useful information on $PCL/CO_2/N_2$ systems, some other relevant points of concern are related to the specific nature of the extrusion process.

Here, the PFA concentration is determined by the different mass flow of the species and not by the saturation pressure. In this case, the residence time distribution and the mixing efficiency affect the solubilization and the foaming agent concentration, thereby limiting the final density of the foam. Due to the complexity of the flow field of melt solution, the control of this step is very difficult and empirical procedures are often used [46].

The pressure drop and the pressure drop rate, which control the nucleation step, depend on the geometry of the nucleation nozzle and on the volumetric flow rate of the molten solution. Differently from the batch process, the pressure drop and pressure drop rate can be modulated independently of an applied saturation pressure. Hence, in extrusion foaming, the desired pressure evolution of the system and the desired concentration of the PFA can be imposed independently. In this way, due to improved control of process variables, it is possible to obtain foams characterized by high density and fine morphology. Conversely, in the case of batch process, where the saturation

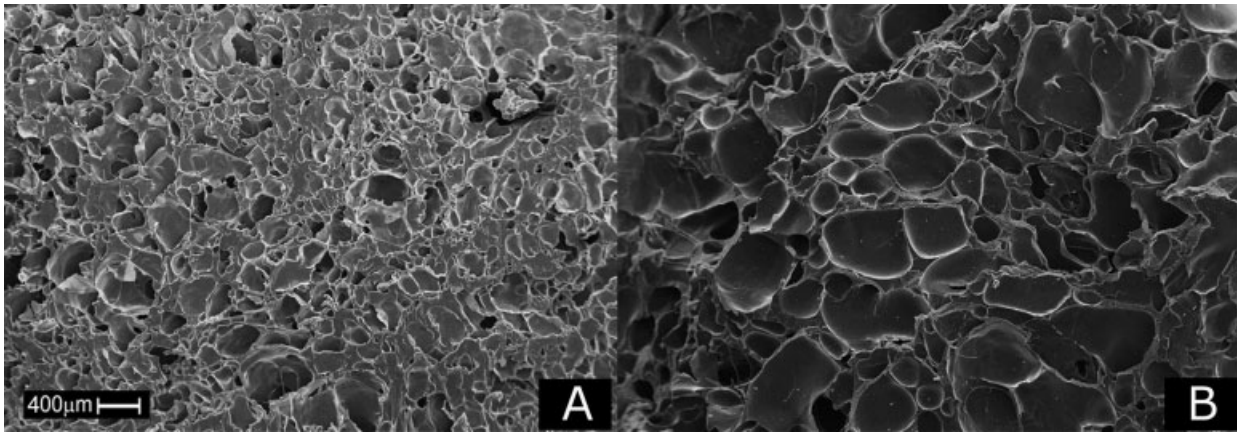

FIG. 8. SEM analysis of PCL extrusion-foamed with CO_2: effect the nucleation nozzle geometry (see text for details).

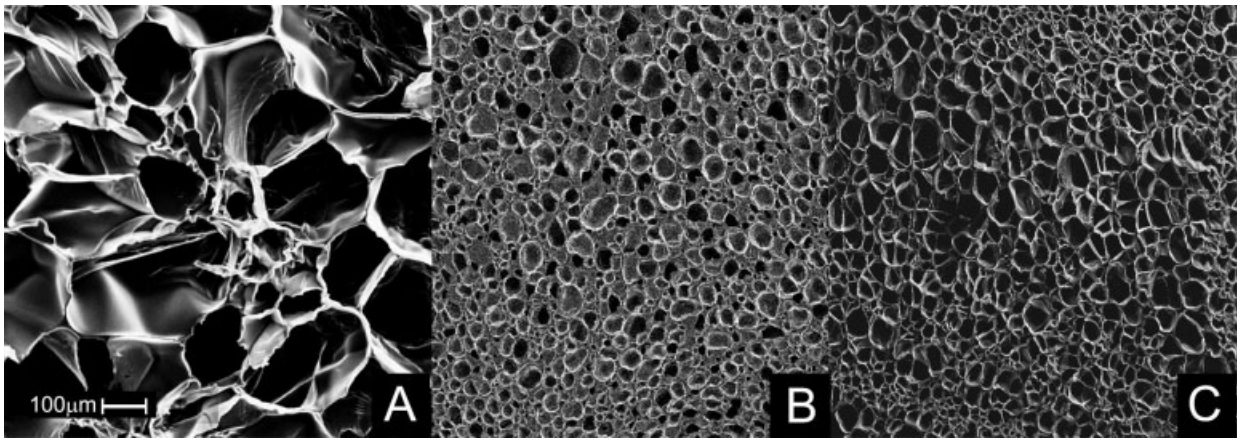

FIG. 9. SEM analysis of PCL extrusion-foamed with CO_2 (A), N_2 (B) and 20/80% CO_2/N_2 mixture (C).

pressure also limits the pressure drop, a low saturation pressure which has to be used to achieve high density-foams leads to structures with poor morphology.

Experimental tests, performed by changing the configuration of the capillary (length and diameter), showed that the nucleation rate varied, as a consequence of the different pressure drop. Therefore, PCL/CO_2 foams, prepared with the longer capillary (l = 30 mm, diameter = 2 mm, ΔP = 120 bar, Fig. 8A), had a finer cellular structure with an average diameter of cells d = 80 μm, as compared to those obtained by using a shorter one (l = 10 mm, diameter = 2 mm, ΔP = 40 bar, Fig. 8B), which had an average diameter of cells d = 300 μm. It is worth noting that the density of the foams was the same, i.e., 0.3 g/cm^3. Morphologies of these two types of foam are reported in Fig. 8.

To lower the densities, higher gas concentrations were used. The optimized procedure led to foam characterized by a density of 0.05 g/cm^3 and mean cell diameter of 200 μm, with the following temperature profile, from the hopper to the die: 90, 100, 100, 100, 70, and 40°C.

Higher uniformity of cell structure but higher densities were achieved with N_2 as foaming agent, by using T_{die} = 45°C. The minimum mean cell diameter was 50 μm with a density of 0.3 g/cm^3.

Best results in term of morphology and density were achieved using as foaming agent in the extrusion a 20–80 wt% CO_2-N_2 mixture: foams were obtained characterized at the same time by a low density (0.15 g/cm^3) and a fine morphology (average cell diameter, d = 20 μm). The morphologies of the extruded foams are shown in the SEM micrographs reported in Fig. 9.

CONCLUSIONS

PCL foams were obtained by using CO_2 and/or N_2 as foaming agents. The different interaction of the two gases with the polymer melt led to different morphology, in terms of foam density, cell number density, and cell size. Compared to N_2, CO_2 was much more soluble and plasticized the polymer more efficiently. In the batch and the extrusion processes this means lower foaming temperature and lower densities. Foams with densities of 0.03 g/cm^3 were produced at 30°C with CO_2, while at least 40°C were used with N_2 (minimum density was 0.24 g/cm^3). Foam optimization based on the use of the mixture of the two gases led to a low-density microcellular structure. In addition, it has been shown how it is possible to achieve the production of a foam structure that meets the application requirements by tailoring the composition of the expanding gas mixtures.

REFERENCES

1. D. Klempner and K.C. Frisch, *Polymeric Foams*, Hanser, New York (1991).
2. J.L. Throne, *Thermoplastic Foams*, Sherwood Publishers, Hinckley, OH (1996).
3. S.-T. Lee, *Foam Extrusion*, Technomic Publishing Co. Inc., Lancaster, PA (2000).
4. J.S. Colton and N.P. Suh, *Polym. Eng. Sci.*, **27**, 485 (1987).
5. J.S. Colton and N.P. Suh, *Polym. Eng. Sci.*, **27**, 493 (1987).
6. C.D. Han and C.A. Villamizar, *Polym. Eng. Sci.*, **18**, 687 (1978).
7. J.H. Han and C.D. Han, *J. Polym. Sci., Part B: Polym. Phys.*, **30**, 711 (1990).
8. J.H. Han and C.D. Han, *J. Polym. Sci., Part B: Polym. Phys.*, **30**, 743 (1990).
9. A. Arefmanesh and S.G. Advani, *Polym. Eng. Sci.*, **35**, 252 (1995).
10. A. Arefmanesh and S.G. Advani, *Rheol. Acta*, **30**, 274 (1991).
11. S.K. Goel and E.J. Beckman, *AIChE J.*, **41**, 357 (1995).
12. K. Joshi, J.G. Lee, M.A. Shafi, and R.W. Flumerfelt, *J. Appl. Polym. Sci.*, **67**, 1353 (1998).
13. J.S. Vrentas and C.M Vrentas, *J. Appl. Polym. Sci.*, **67**, 2093 (1998).
14. A.A. Ahmadi and P.R. Hornsby, *Plas. Rubber Proc. Appl.*, **5**, 35 (1985).
15. A.A. Ahmadi and P.R. Hornsby, *Plas. Rubber Proc. Appl.*, **5**, 51 (1985).

16. D.N. Bikiaris and G.P. Karayannidis, *J. Polym. Sci.: Part B: Polym. Phys.*, **34**, 1337 (1996).
17. D.N. Bikiaris and G.P. Karayannidis, *J. Appl. Polym. Sci.*, **60**, 55 (1996).
18. H.C. Lau, S.N. Bhattacharya, and G.J. Field, *Polym. Eng. Sci.*, **38**, 1915 (1998).
19. C.B. Park, A.H. Behravesh, and R.D. Venter, *Polym. Eng. Sci.*, **38**, 1812 (1998).
20. C.B. Park and L.K. Cheung, *Polym. Eng. Sci.*, **37**, 1 (1997).
21. J.J. Park, L. Katz, and N.G. Gaylord, U.S. Patent 5,116,881 (1992).
22. D.C. Venerus and N. Yala, *AIChE J.*, **43**, 2948 (1997).
23. F. Yoshii, K. Makuuchi, S. Kikukawa, T. Tanaka, J. Saitoh, and K. Koyama, *J. Appl. Polym. Sci.*, **60**, 617 (1996).
24. C.B. Park, D.F. Baldwin, and N.P. Suh, *Polym. Eng. Sci.*, **35**, 432 (1995).
25. C.B. Park, "Continuous Production of High-Density and Low-Density Microcellular Plastics in Extrusion," in *Foam Extrusion*, S.-T. Lee, editor, Technomic Publishing Co., Inc., Lancaster, PA, 263 (2000).
26. C.P. Park, "Polyolefin Foam," in *Polymeric Foam*, D. Klempner and K.C. Frisch, editors, Hanser, New York, 187 (1991).
27. W. Ruengphrathuengsuka, "Bubble Nucleation and Growth Dynamics in Polymer Melts," Ph.D. thesis, Texas A&M University College Station, TX (1992).
28. S. Cotugno, E. Di Maio, C. Ciardiello, S. Iannace, G. Mensitieri, and L. Nicolais, *Ind. Eng. Chem. Res.*, **42**, 4398 (2003).
29. D.I. Collias and D.G. Baird, *Polym. Eng. Sci.*, **35**, 1167 (1995).
30. D.I. Collias and D.G. Baird, *Polym. Eng. Sci.*, **35**, 1178 (1995).
31. J.S. Colton and N.P. Suh, *Polym. Eng. Sci.*, **27**, 500 (1987).
32. L.J. Gerhardt, A. Garg, C.W. Manke, and E. Gulari, *J. Polym. Sci.: Part B: Polym. Phys.*, **36**, 1911 (1998).
33. L.J. Gerhardt, C.W. Manke, and E. Gulari, *J. Polym. Sci.: Part B: Polym. Phys.*, **35**, 523 (1997).
34. J.S. Chiou, J.W. Barlow, and D.R.J. Paul, *J. Appl. Polym. Sci.*, **30**, 3911 (1985).
35. J.S. Chiou, J.W. Barlow, and D.R.J. Paul, *J. Appl. Polym. Sci.*, **30**, 2633 (1985).
36. J.R. Royer, Y.J. Gay, J.M. De Simone, and S.A. Khan, *J. Polym. Sci.: Part B: Polym. Phys.*, **38**, 3168 (2000).
37. R.K. Jain and R. Simha, *Macromolecules*, **17**, 2663, (1984).
38. V.S. Nanda, R. Simha, and T. Somcinsky, *J. Polym. Sci.: Part C*, **12**, 277 (1966).
39. J.S. Vrentas, J.L. Duda, and A.C. Hou, *J. Polym. Sci.: Part B: Polym. Phys.*, **33**, 2581 (1987).
40. K. Mizoguchi, T. Hirose, Y. Naito, and Y. Kamiya, *Polymer*, **28**, 1298 (1987).
41. Y.P. Handa, S. Capowski, and M. O'Neill, *Thermochim. Acta*, **226,** 177 (1993).
42. E. Beckman and R.S.J. Porter, *J. Polym. Sci.: Part B: Polym. Phys.*, **25**, 1511 (1987).
43. Z. Zhang and Y.P. Handa, *Macromolecules*, **30**, 8499 (1997).
44. Y.P. Handa, Z. Zhang, and B. Wong, *Macromolecules*, **30**, 8505 (1997).
45. Ph.T. Jaeger, R. Eggers, and H. Baumgartl, *J. Supercrit. Fluids*, **24**, 203 (2002).
46. M. Lee, C.B. Park, and C. Tzoganakis, *Polym. Eng. Sci.*, **39**, 99 (1999).